Anderson impurity in the one-dimensional Hubbard model on finite size systems

S. Costamagna, C. J. Gazza, M. E. Torio, and J. A. Riera
Instituto de Física Rosario, Consejo Nacional de Investigaciones Científicas y Técnicas, Universidad Nacional de Rosario, Rosario, Argentina
(Dated: February 6, 2008)

An Anderson impurity in a Hubbard model on chains with finite length is studied using the density-matrix renormalization group (DMRG) technique. In the first place, we analyzed how the reduction of electron density from half-filling to quarter-filling affects the Kondo resonance in the limit of Hubbard repulsion $U = 0$. In general, a weak dependence with the electron density was found for the local density of states (LDOS) at the impurity except when the impurity, at half-filling, is close to a mixed valence regime. Next, in the central part of this paper, we studied the effects of finite Hubbard interaction on the chain at quarter-filling. Our main result is that this interaction drives the impurity into a more defined Kondo regime although accompanied in most cases by a reduction of the spectral weight of the impurity LDOS. Again, for the impurity in the mixed valence regime, we observed an interesting nonmonotonic behavior. We also concluded that the conductance, computed for a small finite bias applied to the leads, follows the behavior of the impurity LDOS, as in the case of non-interacting chains. Finally, we analyzed how the Hubbard interaction and the finite chain length affect the spin compensation cloud both at zero and at finite temperature, in this case using quantum Monte Carlo techniques.

PACS numbers: 73.23.-b, 73.21.La, 72.15.Qm, 71.27.+a

I. INTRODUCTION

There is an increasing interest in strongly correlated systems containing onedimensional (1D) structures, both for their novel properties as well as for their possible applications. For example, chains and two-leg ladders are present in transition metal oxides and in organic conductors. Other systems of increasing interest involving strongly correlated features are nanoscopic devices which have been recently fabricated and experimentally studied.[1] In many of these devices, a droplet of electrons confined in the three spatial directions, the quantum dot (QD), is connected to metallic leads. In this case the leads are described by tight-binding models, or in general by Fermi liquids. The transport through such devices involve the formation of a Kondo resonance in the QD. Kondo physics is then relevant to understand this kind of devices.[2]

It is also possible to connect the QD to conducting leads with electron correlations. This is the case of spin valves, one of the simplest devices used in spintronics,[3,4] where a QD is attached to ferromagnetic leads. These leads can be built from materials such as manganese oxides[5] or other compounds containing transition metal oxides such as vanadates.[6] There have also been recent developments in producing devices where the leads are formed by carbon nanotubes (although ultimately these leads are connected to metallic terminals) which can be considered quasi-onedimensional and where electron correlations are presumably important.[7,8,9] In fact, a Luttinger liquid behavior, typical of correlated 1D systems, has been found in carbon nanotubes.[10]

The problem of a magnetic impurity or QD in a correlated onedimensional system is then an interesting topic both for fundamental and for technological reasons. From the theoretical point of view, the most important results for this kind of systems were obtained by considering a single impurity attached to leads described by Luttinger liquids. Much less is known when the leads are described by a Hubbard model. In this case, this model has been treated by linearizing the dispersion relation and, using bosonization techniques, the long wavelength behavior is captured. Within this approach, it was shown that in a system of a magnetic impurity connected to Luttinger chains by a Kondo exchange interaction J, the Kondo temperature acquires the power-law expression[11] $T_K \approx (J)^{2/(1-K_\rho)}$ instead of the conventional exponential law for noninteracting chains. The Luttinger exponent K_ρ also determines the conductance through an interacting wire, which is given by $G = 2K_\rho e^2/h$.[12]

In this article we consider the even less studied problem of a single-impurity Anderson-Hubbard Hamiltonian on finite-size systems. Our aim is to provide a detailed microscopic picture of the competition between the electron correlations on the impurity and the ones on the leads, and to understand the role of finite length of the chains. Although the lengths considered in this study are still smaller than the physical length of current devices, the study on finite-size systems are interesting per se. In fact, it has been suggested that the Kondo temperature can be very different in finite chains with respect to the one in infinite leads.[13] It is also expected that the size of nanoelectronic devices will be further reduced in the near future. The fundamental problem of the competition between the Kondo effect and the Luttinger liquid starting from a microscopic Hamiltonian was recently studied on infinite systems using an approximated analytical renormalization group technique.[14] The problem of an Anderson impurity in a $t - J$ model has been also addressed within the Bethe *Ansatz* formalism.[15]

Although manganese oxides should be described by

a generalized ferromagnetic Kondo-lattice model[16], and vanadates or carbon nanotubes by some variants of the Hubbard or $t-J$ models on ladders[17,18], in order to get an insight on the physical behavior, it is necessary to consider first the simpler case of leads described by a 1D Hubbard model. Of course, some of the results obtained are relevant to magnetic impurities in strongly correlated quasi-1D compounds such as those mentioned at the beginning. Results for LDOS for example, could be compared with those obtained by scanning tunneling microscopy (STM) experiments.[19]

Numerical techniques are ideally suited to cope with finite systems. In particular we mainly employ the DMRG technique,[20] which provides essentially exact results for various real-space properties on finite chains. These real-space properties of real-space models can shed light on the functioning of QD devices.[21] In this sense, in this work we will determine the way in which the Kondo effect is affected by varying the electron density or the Hubbard repulsion on the leads by computing the electron occupation and the square of the z-component of the spin at the impurity site. More importantly, from the spin-spin correlation functions we will study the "spin compensation cloud", a possible measure of the more elusive Kondo screening cloud.[22] Using this technique, it has been shown that the screening cloud is reduced by electron correlations on the leads in a system with two Kondo impurities.[23] We will extend this approach to the Anderson impurity where we will make a careful study of finite-size effects. DMRG results for the spin compensation cloud have been reproduced to a good approximation by using a recently developed quantum Monte Carlo technique[24]. This technique also allows us to study this quantity at finite temperature.

In order to study transport properties, we will study the LDOS at the impurity, which is related to the conductance in an essential way. By implementing some recent developments in DMRG[27,28], we will compute the conductance as the response of the system to a finite but small voltage bias applied to the leads. We will examine this property as the Hubbard repulsion U is varied. We will also show that the effect of this variation on both the LDOS at the impurity and the conductance, depend in turn on the values of the electron interactions on the impurity. We will explore various types of impurities, from the mixed valence to Kondo regimes.

The paper is organized as follows. In Section II we describe the model studied and we provide details of the numerical techniques employed. In Section III we study the effect of reducing the electron density from half-filling to quarter-filling for the case of noninteracting (tight-binding) leads. In Section IV, we analyze how the Kondo effect varies with the Hubbard repulsion U on the leads at quarter-filling. Finally, the relation between the results obtained and those in the previous literature, and the relevance of the present study to real systems or nanoscopic devices, are discussed in Section V.

II. MODEL AND METHODS

In this paper we use the terms "impurity" and QD indistinctly, and we refer to the remainder sites of the chain as the "leads". We consider a one-dimensional single-impurity Anderson-Hubbard model defined by the Hamiltonian:

$$\begin{aligned}\mathcal{H} = &- t\sum_{i=\leq -2,\sigma}(c^{\dagger}_{i\sigma}c_{i+1\sigma}+H.c.)+U\sum_{i=\leq -1}n_{i,\uparrow}n_{i,\downarrow}\\ &- t\sum_{i=\geq 1,\sigma}(c^{\dagger}_{i\sigma}c_{i+1\sigma}+H.c.)+U\sum_{i=\geq 1}n_{i,\uparrow}n_{i,\downarrow}\\ &- t'\sum_{\sigma}(c^{\dagger}_{-1\sigma}c_{0\sigma}+c^{\dagger}_{0\sigma}c_{1\sigma}+H.c.)\\ &+ \epsilon'\ n_0+U'n_{0,\uparrow}n_{0,\downarrow} \qquad (1)\end{aligned}$$

where conventional notation was used. The first two terms correspond to the left lead and the following two terms to the right lead. The next term is the impurity-lead interaction, and the last two terms are the on-site energy and Hubbard repulsion at the impurity site, located at site 0, respectively. We adopt t as the scale of energy. In the case of $U=0$, the Hamiltonian (1) reduces to the single-impurity Anderson model, and for $\epsilon'=0$, $U'=U$, $t'=t$, to the Hubbard model.

Hamiltonian (1) will be studied mostly using the numerical technique DMRG[20,25] on finite-size clusters of length L with open boundary conditions (OBC). This algorithm provides numerically exact results for static properties at zero temperature with a precision which depends on the number M of states retained. Most of the results here reported were obtained for $M=600$, except otherwise stated, asserting us that the integrated weight of discarded states are of order 10^{-6} in the worst case. On the other hand, results for dynamical properties, such as LDOS, should be taken qualitatively, as discussed below. The same apply to the results obtained for the time evolution of the current on the links connecting the impurity with the leads. In order to assess even-odd effects most of the results reported below were obtained by using even and odd chain lengths. Throughout all this paper, DMRG calculations will be done in the subspace of total $S_z=0$ ($S_z=1/2$) for L even (odd). The QD is located in one of two central sites of the chain when L is even (in the central site when L is odd).

We have computed static properties such as the electron occupancy on each site, $\langle n_{i,\sigma}\rangle$ ($\sigma=\uparrow,\downarrow$) and spin-spin correlations from the QD, $S(j)=\langle S^z_0\ S^z_j\rangle-\langle S^z_0\rangle\langle S^z_j\rangle$.

A very important quantity related to the Kondo effect is the Kondo screening length, which is somewhat elusive to compute.[13] A possible measure of this Kondo length is the length of the "spin compensation cloud"[22] defined as the length ξ such that

$$\sum_{j=-\xi/2,j\neq 0}^{j=\xi/2} S(j)=xS(0), \qquad (2)$$

where x is an arbitrary parameter. In the following we adopt a fixed value $x = 0.9$ in order to compare ξ for the different cases.

One of the main quantities we have studied is the local density of states, $\rho(\omega)$, at the QD. In the first place, from this quantity it would be possible to evaluate the conductance in the linear response regime (see below). In the second place, recent advances in STM have made it possible to directly measure this quantity. Since in our DMRG calculation the measurements are performed when the two added sites are at the center of the chain (symmetrical configuration), the QD then is one of these two sites which are exactly treated. Then, we adopt the approximation of applying the creation and annihilation operators at the QD on the ground state vector and then determine $\rho(\omega)$ following the well-known continued fraction formalism. A more accurate approach would be, after the application of each of those creation and annihilation operators, to run additional sweeps for an enlarged density matrix.[26] In any case, the truncation of the Hilbert space is the essential source of error in DMRG, and to estimate the precision of our approach we have compared results for various numbers of retained states M, from $M = 300$ to 600. We would also like to stress the fact that the conductance in linear response is related to the LDOS near $\omega = 0$ where the approximation is more precise. Our calculation starts to be less precise as we move away from the chemical potential, since then higher excited states are involved.

For this kind of systems, specially in connection to nanoscopic devices, the most interesting properties are those related to transport, in particular, the conductance G. When the chains or leads are described by a tight-binding model, or in general by a Fermi liquid, various expressions relating it to the LDOS at the impurity are available in linear response, as mentioned before. In addition, the Friedel's sum rule (see Eq. (7) below) allows a simple and precise calculation of G, particularly for numerical techniques. In the case of Hubbard chains, or in general Luttinger liquid leads, one must resort to the expression, in linear response,[12]

$$G = \lim_{\omega\to 0} \frac{1}{\hbar L\omega} \int_0^L \int dx\ dt\ e^{i\omega t} \langle J(x,t)J(0,0)\rangle \qquad (3)$$

where the current is defined as

$$J(x,t) = i\frac{e}{\hbar} t_x \sum_\sigma \langle \Psi(t)|(c^\dagger_{x+1\sigma} c_{x\sigma} - H.c.)|\Psi(t)\rangle, \qquad (4)$$

and $|\Psi(t)\rangle$ is the ground state of the system at time t.

Although such a calculation can be carried out within DMRG, some recent developments collectively known as time-dependent DMRG[27,28] allow to compute directly $\langle J(x,t)\rangle$ as $\langle \Psi(t)|J(x)|\Psi(t)\rangle$. The time-evolution is triggered by the application of a bias voltage ΔV between the left and right leads at $t = 0$.[29,30] That is, at time $t = 0$, a potential $-\Delta V/2n_i$ ($\Delta V/2n_i$) on the sites on the left (right) leads is switched on. Then, charge moves from one lead to the other in a non-equilibrium process. This non-equilibrium process was studied analytically in Ref. 31. In finite size systems, $\langle J(x,t)\rangle$ follows an oscillatory evolution as charge is bounced between the left and right leads. As the length of the leads are extended to infinity, the period of this oscillation becomes infinitely long (the leads become infinite charge reservoirs) and the usual concept of conductance is recovered. It was shown in Refs. 29,30 that even for moderate size clusters, on each period, $\langle J(x,t)\rangle$ reaches a plateau that corresponds to the value of the bulk limit. Hence a measure of the conductance can be obtained as the value of this plateau or the amplitude of this oscillation, that is:

$$G(\Delta V) = \max_t \frac{\langle J(t)\rangle}{\Delta V} \qquad (5)$$

where

$$J(t) = (J_L(t) + J_R(t))/2 \qquad (6)$$

and $J_L(t)$ ($J_R(t)$) is the current on the link connecting the impurity site with the left (right) lead. Notice that Eq. (5) is valid for an arbitrary finite bias ΔV. The evolution of the ground state $|\Psi(t)\rangle$ from t to $t + \Delta t$ is computed with a *static* Runge-Kutta treatment of the time-dependent Schrödinger equation.[32] Again in this case, a much precise calculation could be performed by including $|\Psi(t)\rangle$ at intermediate times τ as targeted states in the density matrix and by running additional sweeps.[27] This approach is of course much more expensive computationally.

In the calculations reported below we adopted a bias $\Delta V = 0.01$ and a time step $\Delta t = 0.1$.

Finally, we report finite temperature results obtained with quantum Monte Carlo simulations using the stochastic series expansion (SSE) algorithm.[24] In this case, we consider chains with periodic boundary conditions (PBC). The use of PBC helps to assess the effects of the Friedel oscillations which appear with OBC, used with DMRG, but are absent with PBC. SSE with the loop upgrade is a very efficient QMC algorithm which allows to reach much lower temperatures and larger sizes than other QMC algorithms. It also avoids the problem of extrapolation of the Trotter dimension common in "world-line" algorithms. It is also worth to note that SSE works in the grand canonical ensemble, i.e., the chemical potential has to be tuned to give a desired density *on average*. Notice that the "minus sign problem" which affects quantum Monte Carlo simulations for fermionic models is absent in 1D with hopping between nearest neighbor sites only since fermion permutations appear just as a boundary effect.

III. NONINTERACTING LEADS, ELECTRON DENSITIES AWAY FROM HALF-FILLING

The main purpose of this work is to study the effects of correlations on the leads. This study will be performed

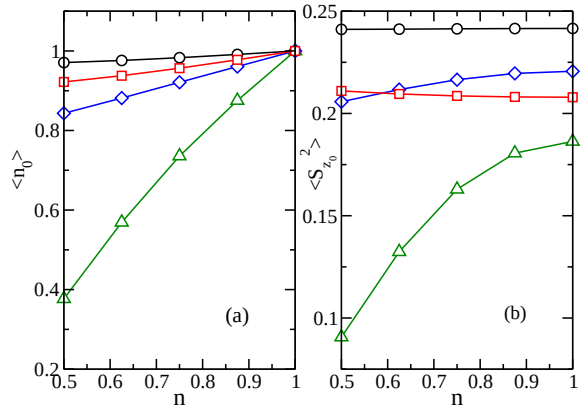

FIG. 1: (Color online) (a) Electron occupancy and (b) $\langle S_z^2 \rangle$ at the impurity site as a function of the filling for $U' = 8$, $t' = 0.5$ (circles), $U' = 8$, $t' = 1.0$ (squares), $U' = 4$, $t' = 0.5$ (diamonds) and $U' = 2$, $t' = 0.5$ (triangles). $L = 96$

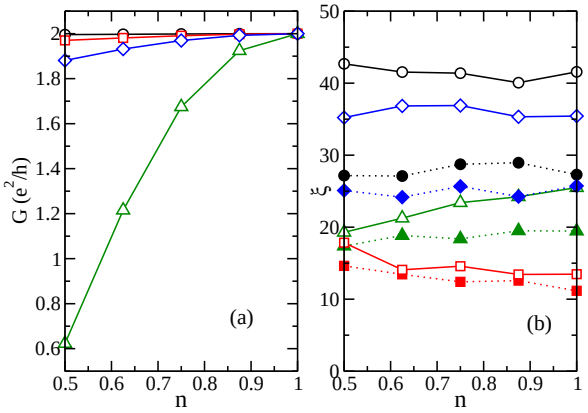

FIG. 2: (Color online) (a) Conductance obtained from the Friedel's sum rule, and (b) length of the compensation cloud ξ, as a function of the filling for $U' = 8$, $t' = 0.5$ (circles), $U' = 8$, $t' = 1.0$ (squares), $U' = 4$, $t' = 0.5$ (diamonds) and $U' = 2$, $t' = 0.5$ (triangles). $L = 64$ (full symbols, dot lines), $L = 96$ (open symbols, full lines).

in the next Section. Most theoretical studies on Kondo effect have considered the half-filled case ($n = 1$), where the system is particle-hole symmetric. Now, since an infinitesimal value of U drives the system into an insulating state, in order to keep the leads metallic in the presence of correlations it is necessary to study the system away from half-filling. In Section IV we will work at quarter-filling ($n = 0.5$). In this Section, as a preliminary step, we study the evolution of the Kondo effect as the filling is reduced from $n = 1$ to $n = 0.5$ in the absence of interactions on the lead ($U = 0$). In particular we are interested in following the evolution of what at half-filling is the Kondo resonance, as the electron density decreases.

Model Eq.(1), which as stated above reduces to the single-impurity Anderson model, was studied by DMRG for several L up to 96 sites, and for fillings $n = 1$, 0.875, 0.75, 0.625 and 0.5. Since, as we said in the Introduction, there is a competition between the correlations on the leads and the correlations at the impurity or QD, we consider four sets of interactions on the impurity: $\{U' = 8, t' = 0.5\}$, $\{U' = 8, t' = 1.0\}$, $\{U' = 4, t' = 0.5\}$, and $\{U' = 2, t' = 0.5\}$. In all cases we consider the symmetric case, $\epsilon' = -U'/2$. For these sets of parameters, the effective Kondo coupling $J_{eff} = 4t'^2/U'$ takes the values 0.125, 0.5, 0.25, and 0.5 respectively, although strictly this relationship is only valid for $U' >> t'$, and hence not much applicable to the last case. In spite of sharing the same J_{eff}, the second and fourth sets behave quite differently as we will show below.

Let us start by examining the dependence of the electron occupancy $\langle n_0 \rangle$ and $\langle S_{z,0}^2 \rangle$ at the impurity site with the electron density. This variation depends in turn strongly on the interactions at the impurity as it can be seen in Fig. 1. If $\langle n_0 \rangle = 1$, $\langle S_{z_0}^2 \rangle$ takes its maximum value (1/4) when the impurity is a perfect spin-1/2, corresponding to the full Kondo regime. In the mixed valence regime, it takes the value 1/12. For the parameter set $\{U' = 8, t' = 0.5\}$, the system is in a well defined Kondo regime, and the dependence with n is relatively weak. On the opposite case, for $\{U' = 2, t' = 0.5\}$ the system is not in a well-defined Kondo regime at half-filling, and the dependence with the electron filling is stronger. The reduction of electron density drives the system into the mixed valence regime. Notice that in this second case, the occupancy of the impurity is smaller than n. Besides, it is well known that there are Friedel oscillations in $\langle n_i \rangle$ beginning at the ends of the chains with OBC.[33] It is then valid to ask if these oscillations could have some effect on the electron occupancy at the impurity. In the present case, any important influence of the Friedel oscillations on the impurity properties can be ruled out because the results for $L = 96$ are virtually identical within error bars to those obtained with SSE and using PBC where these oscillations are absent, at the lowest temperatures we considered. Of course, the presence of the impurity induces other density oscillations which overimpose to the Friedel oscillations induced by the open ends. In fact we have observed in some cases that the presence of the impurity changes the period of the open end oscillations from $2k_F$ to $4k_F$. This issue is worth to be examined more thoroughly but it is somewhat outside the scope of the present work.

From the values of the electron occupancy it is possible to obtain the conductance by using the Friedel's sum rule:[2,34]

$$G_\sigma = sin(\pi n_\sigma)^2 \qquad (7)$$

($\sigma = \uparrow, \downarrow$) which is valid when the bandwidth is much larger than the Kondo coupling. Results for $G = G_\uparrow + G_\downarrow$ are shown in Fig. 2(a), for the four types of impurities considered. As expected from the results in Fig. 1(a), the conductance decreases by reducing electron density from half-filling.

The length of the spin compensation cloud ξ is de-

picted in Fig. 2(b) for the same four types of impurities. ξ depends on two factors: (i) the effective exchange coupling between the magnetic impurity and the spins of the conduction electrons, and (ii), to a lesser extent, how much defined is the magnetic character of the impurity or the Kondo regime. The finite length of the cluster imposes an upper bound to the compensation length. It has been pointed out that the inability of the finite system to accommodate the Kondo cloud would modify in turn the Kondo effect, in particular the Kondo temperature.[13] For the parameter set $U' = 8$, $t' = 0.5$ ($J_{eff} = 0.125$) the compensation cloud is large, quite likely exceeding the system size since $\xi \approx L/2$, and scaling linearly with the system size. For $U' = 4$, $t' = 0.5$ ($J_{eff} = 0.25$), ξ is somewhat smaller but still scales linearly with L. On the other hand, for the $U' = 8$, $t' = 1$ ($J_{eff} = 0.5$) impurity, where $\langle S^2_{z,0}\rangle \approx 0.21$, the length of the compensation cloud is much smaller and it has a weak dependence with L. An intermediate situation occurs for the fourth type of impurity, $U' = 2$, $t' = 0.5$ which has the same $J_{eff} = 0.5$ but with a poorly defined magnetic character ($\langle S^2_{z,0}\rangle < 0.2$), leading to a more extended compensation cloud. Notice an overall weak dependence of ξ with the electron density.

It is important to understand the behavior of the conductance shown in Fig. 2(a) by studying the LDOS at the impurity site, $\rho(\omega)$. In Fig. 3 we show $\rho(\omega)$ close to the Fermi level, for the four types of impurities and for several electron densities from half-filling to quarter-filling. $\rho(\omega)$ has been shifted to the chemical potential μ for the sake of comparison, since starting from half-filling, μ shifts to $\omega < 0$. In this figure and all the following similar ones, we adopted a Lorentzian broadening of the peaks of $\delta = 0.1$. A measure of the precision of the results presented can be inferred from the comparison between $L = 95$, $M = 500$, and $L = 96$, $M = 300$. Clearly, the main features are present in both cases but it can be seen that the ones for $L = 95$, $M = 500$ are more consistent as n is reduced. For the impurity $U' = 8$, $t' = 0.5$, the Kondo peak at half-filling remains at the Fermi level upon reducing the density down to $n = 0.5$. This is consistent with the relative large conductance of this case. For the impurity $U' = 8$, $t' = 1$, the peak shifts slightly away from resonance as the filling is reduced, going into the electron part of the spectrum ($\omega - \mu < 0$). Also in this case, the behavior of $\rho(0)$ is correlated with the conductance weakly varying with the density. For these two impurities, the Coulomb or holon peaks fall outside of the frequency range adopted in the plot. In the case of $U' = 4$, $t' = 0.5$, the Coulomb peak at $\omega \approx -U/2$ shows up as n decreases. The overall behavior of the Kondo peak is similar to that of the first impurity and this is related to the small J_{eff} of these cases. On the other hand, for the case $U' = 2$, $t' = 0.5$, the chemical potential shifts *below* the Coulomb peak at $\omega \approx -U/2$ (the Coulomb peaks are those located at $\omega - \mu \sim \pm 1$ at half-filling). This behavior is clearly correlated with the important suppression of the conductance for this impurity observed in Fig. 2(a).

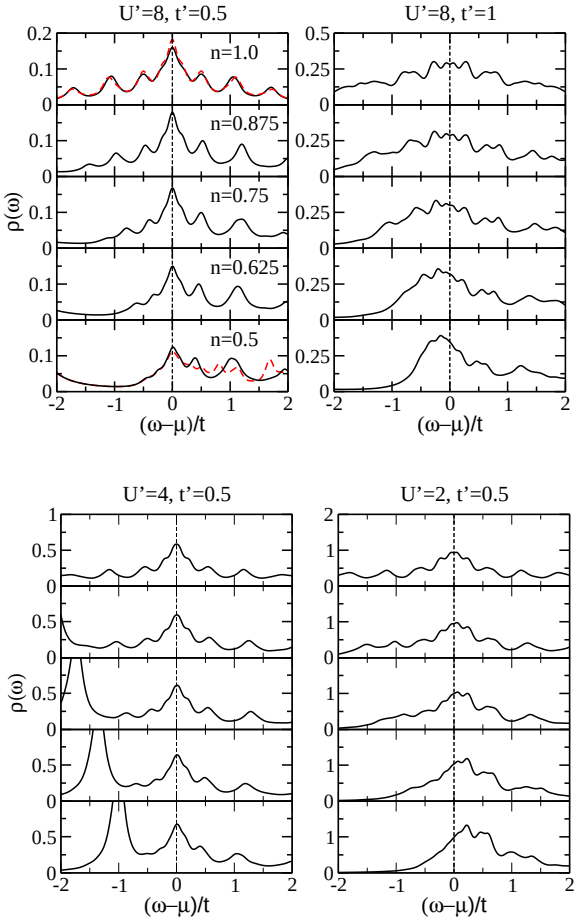

FIG. 3: (Color online) Evolution of the LDOS at the impurity site as the electron density is reduced from half-filling to quarter-filling. Titles on each panel show the corresponding impurity parameters. For each panel, the fillings are $n = 1.0$, 0.875, 0.75, 0.625 and 0.5 from top to bottom, $L = 95$, $M = 500$. Dashed lines in the top left panel correspond to $L = 96$, $M = 300$

For the $U' = 8$, $t' = 1$, and $U' = 2$, $t' = 0.5$ impurities, the observed splitting of the central peak at $n = 1$ is just a finite size effect; the split between the two central peaks, which correspond to electron creation ($\omega - \mu > 0$) and annihilation ($\omega - \mu < 0$), close when $L \to \infty$. Notice also the different amplitudes of the spectral weight at the Fermi level, roughly proportional to J_{eff}.

IV. INTERACTING LEADS, QUARTER-FILLING

After examining the effect of varying the filling in a system with an Anderson impurity in a tight-binding chain, we now turn to the central issue of this paper, that is the effect of the presence of a Hubbard on-site potential on the chain. Then, we consider the full Hamiltonian defined in (1), at quarter-filling, and taking $U = 1$, 2, 4 and 8. In the pure Hubbard chain, the system behaves

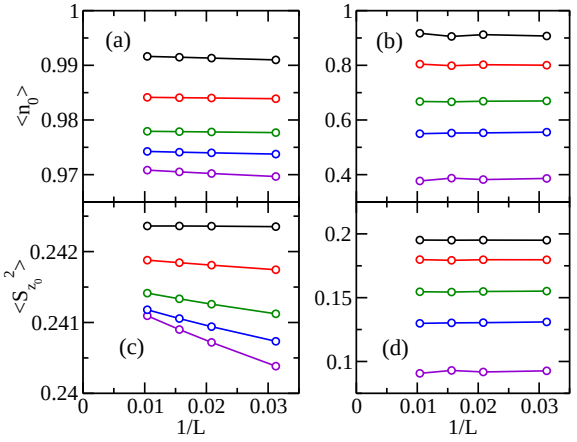

FIG. 4: (Color online) (a),(b) Electron occupancy and (c),(d) $\langle S_z^2 \rangle$ at the impurity site as a function of the inverse of the chain length L for $U = 0$, 1, 2, 4, and 8, from bottom to top. $U' = 8$, $t' = 0.5$ (left panel), $U' = 2$, $t' = 0.5$ (right panel). $n = 0.5$.

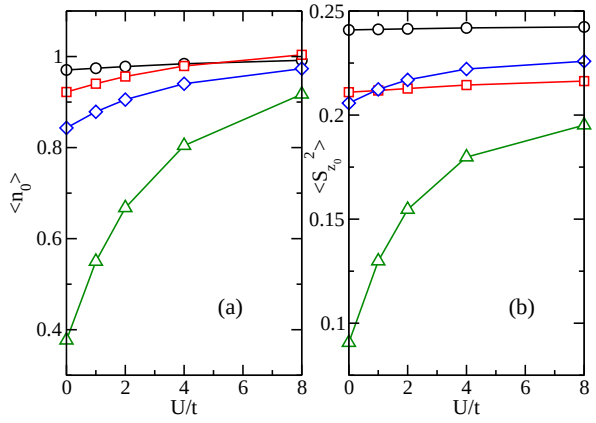

FIG. 5: (Color online) (a) Electron occupancy and (b) $\langle S_z^2 \rangle$ at the impurity site as a function of the interaction on the leads U for $U' = 8$, $t' = 0.5$ (circles), $U' = 8$, $t' = 1.0$ (squares), $U' = 4$, $t' = 0.5$ (diamonds), and $U' = 2$, $t' = 0.5$ (triangles). $L = 96$, $n = 0.5$.

as a Luttinger liquid, and hence, from the point of view of transport properties is a metal.

We start by looking at finite size behavior of the electron occupancy and $\langle S_z^2 \rangle$ at the impurity. Results for the impurities $U' = 8$, $t' = 0.5$ and $U' = 2$, $t' = 0.5$ as a function of $1/L$ are shown in Fig. 4. For each value of U a weak variation can be observed in $\langle n_0 \rangle$. For the case of $U' = 8$, $t' = 0.5$ there is a somewhat larger variation of $\langle S_{z,0}^2 \rangle$ which becomes weaker as U is increased.

The fact that as U increases, both $\langle n_0 \rangle$ and $\langle S_{z,0}^2 \rangle$ increase, is a general behavior observed for all the values of U' and t' that we examined, as can be seen in Fig. 5. Note that for $U' = 8, t' = 1$ in Fig. 5(a) the system reaches the limit of the pure Hubbard model at $U = 8$, with $\langle n_0 \rangle = 1$, while the other cases represent different kind of impurities, with densities not necessarily equal to 1. This forces the crossing of the two $U' = 8$ curves found near $U = 5$. For the cases $U' = 2$ and $U' = 4$, for $U > U'$ we can observe a change in the growing behavior of both $\langle n_0 \rangle$ and $\langle S_{z,0}^2 \rangle$ curves. In other words, a Hubbard repulsion on the chains favors a more defined magnetic character of the impurity. This is particularly apparent for the impurity with parameters $U' = 2$, $t' = 0.5$, which most likely is in a mixed valence state at $U = 0$, as discussed in the previous Section. Again these results are consistent with those obtained with SSE within error bars. One may conjecture that as U increases, the $4k_F$ electron correlations are enhanced forcing an increased occupation at the impurity. The enhancement of $\langle n_0 \rangle$ and $\langle S_{z,0}^2 \rangle$ with U occurs also at density $n = 0.75$ at least for this impurity parameters.

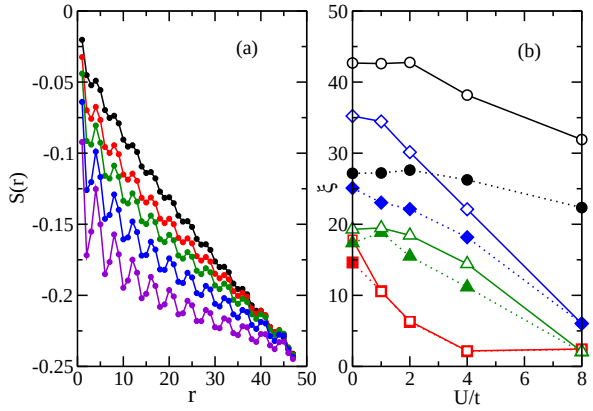

FIG. 6: (Color online) (a) Integral of the spin-spin correlations as a function of the distance from the impurity site (Eq.(2)), $U' = 8$, $t' = 0.5$, and $U = 0$, 1, 2, 4, and 8, from top to bottom; $L = 96$, $n = 0.5$. (b) Length of the compensation cloud as a function of U for the four set of interactions at the impurity, $U' = 8$, $t' = 0.5$, (circles), $U' = 8$, $t' = 1.0$ (squares), $U' = 4$, $t' = 0.5$ (diamonds), and $U' = 2$, $t' = 0.5$ (triangles). $L = 64$ (open symbols), $L = 96$ (filled symbols), $n = 0.5$.

Let us examine now the behavior of the spin compensation cloud when U is increased. In Fig. 6(a), the integral of the spin-spin correlations is plotted as a function of the distance from the impurity. The typical $2k_F$ oscillations which at $n = 0.5$ has a period equal to 4, are clearly seen. $S(r)$ increases (in absolute value) as U increases, implying that the impurity spin becomes screened at shorter distances. This is precisely the behavior of ξ, as it can be seen in Fig. 6(b) for the four types of impurities considered. For $U' = 8$, $t' = 0.5$ and $U' = 4$, $t' = 0.5$ the reduction of ξ with U is clear in spite of the fact that the dependence of ξ with the system size suggests that the bulk limit has not been reached. On the other hand, for $U' = 8$, $t' = 1.0$ and for $U' = 2$, $t' = 0.5$, results for $L = 64$ and 96 are very similar suggesting that the compensation clouds observed are those of the bulk limit. This behavior of the spin compensation cloud is correlated with the increase of $\langle S_{z,0}^2 \rangle$ shown in Fig. 5(b).

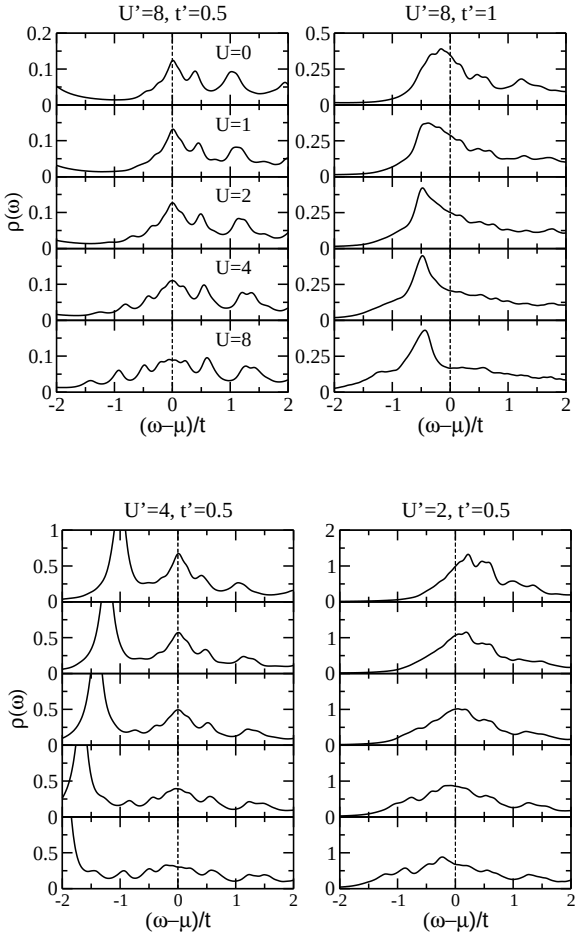

FIG. 7: Evolution of the LDOS at the impurity site as U in the leads is increased. Titles on each panel show the corresponding impurity parameters. For each panel, $U = 0.0$, 1.0, 2.0, 4.0 and 8.0 from top to bottom. $L = 95$, $n = 0.5$.

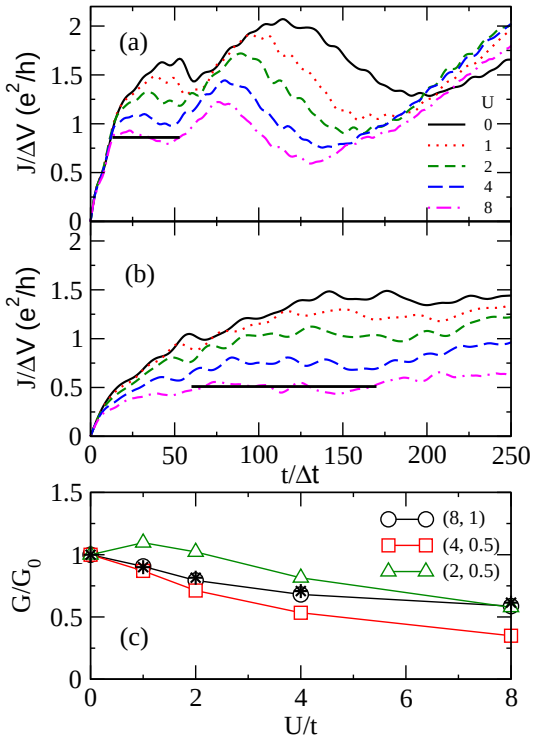

FIG. 8: (Color online) $J(t)/\Delta_V$ for different values of U, (a) $U' = 8$, $t' = 1.0$, (b) $U' = 4$, $t' = 0.5$, $L = 96$, $n = 0.5$, $\Delta V = 0.01$, $\Delta t = 0.1$. The horizontal lines show the time interval over which the average of the current is taken to compute the conductance. (c) Relative conductance (see text) as a function of U for different values of the interactions (U', t'). The values of K_ρ at $n = 0.5$, extracted from Ref.36, are shown with stars.

The relative values of ξ for the various impurities follows in first approximation the values of the Kondo couplings, as was discussed with respect to Fig. 2(b). The overall reduction of ξ with U is consistent with previous calculations for the two-impurity Kondo coupling[23] and expected on general grounds due to the increase of the Kondo temperature with correlations.[11]

The LDOS at the impurity presents also interesting features as U is increased. Let us first consider the impurity $U' = 8$, $t' = 0.5$ (top left panel Fig. 7). In this case the peak retains its resonant character as U increases (only for $U = 8$ it appears at a small negative frequency), and its amplitude is slightly reduced. For the second type of impurity, $U' = 8$, $t' = 1.0$ (top right panel Fig. 7), there is a pronounced transfer of spectral weight to the occupied part of the spectrum, and also $\rho(\omega - \mu = 0)$ is much reduced. For the impurity $U' = 4$, $t' = 0.5$ (bottom left panel), the remains of the Kondo peak stays at the chemical potential, which moves towards positive ω. The same effect of U is observed for $U' = 2$, $t' = 0.5$ (bottom right panel Fig. 7). In this case, the peak located at $\omega - \mu > 0$ for $U = 0$, crosses the Fermi level at $U \sim 4$, and finally appears at $\omega - \mu < 0$ for $U = 8$, as the spectral weight is transfered from the unoccupied to the occupied part of the spectrum. Taking into account the strong enhancement of $\langle S^2_{z,0}\rangle$ for these impurity parameters shown in Fig.5(b), one may conjecture that the states close to the Fermi level that are shifted by increasing U correspond to magnetic excitations becoming increasingly occupied.

Our most relevant results regarding the transport properties in a Hubbard chain in the presence of an Anderson impurity are shown in Fig. 8. In Fig. 8(a,b), we show the average current $J(t)$ on the links connected to the impurity divided by ΔV on a $L = 96$ chain (results for $L = 95$ are virtually identical) for two sets of impurity interactions. As discussed in Section II, $J(t)$ has an oscillatory behavior which is typical of these time-evolving systems.[30,35] The period of these oscillations for the cases shown in Fig. 8 is approximately $800\Delta t$. In this figure, we only show $J(t)$ up to $t = 250\Delta t$ because after that the time-evolution becomes unstable. In some cases, (Fig. 8(a)), these wiggles make the conductance to exceed the value $2e^2/h$ indicating that the time-evolution has already become unstable.

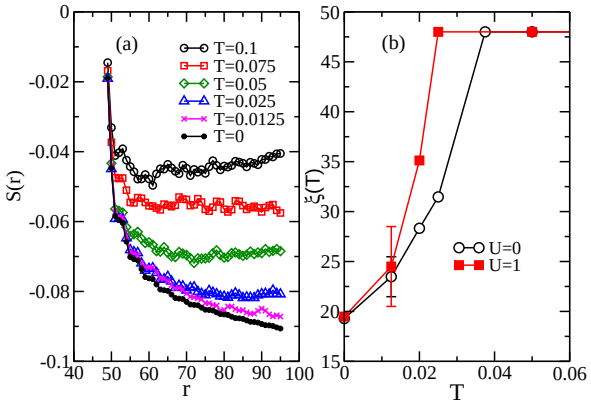

FIG. 9: (Color online) (a) Evolution of the spin compensation cloud as a function of distance from the impurity at various temperatures obtained with SSE, $U' = 2$, $t' = 0.5$, $L = 96$. (b) Length of the spin compensation cloud as a function of temperature $U' = 2$, $t' = 0.5$, $L = 96$, $n = 0.5$, for $U = 0$, and 1. The $T = 0$ values were obtained with DMRG. Error bars are shown for $T = 0.0125$. Temperature in units of t.

From $J(t)/\Delta V$, we have computed the conductance according to Eq. (5). Typical time intervals or "plateaus" over which the time average was taken are shown in Fig. 8(a,b). The values of the conductance $G = G(U)$, for a given impurity, relative to the value for noninteracting leads, $G_0 = G(U = 0)$, are shown in Fig. 8(c). Although there is some arbitrariness in defining these plateaus, a qualitatively clear trend emerges. For the impurities ($U' = 8$, $t' = 1.0$) and ($U' = 4$, $t' = 0.5$) G/G_0 decreases as U increases. In these cases, the suppression is consistent with the reduction of spectral weight at the Fermi level in the impurity LDOS, shown in Fig. 7. In these cases, where a Kondo resonance subsists for finite U, and particularly for ($U' = 8$, $t' = 1.0$), the suppression of the conductance is consistent with the predicted relation[12] $G \sim K_\rho$, as shown in Fig. 8(c). On the other hand, for the case of the impurity parameters $U' = 2$, $t' = 0.5$, G/G_0 follows a more complex behavior. From the non-interacting limit to approximately $U = 1$, G/G_0 increases and then as U increases further, it starts to decrease. This non-monotonous behavior again follows the one of the spectral weight at the Fermi level in the impurity LDOS (Fig. 7, bottom right panel).

Finally, we report a finite temperature study of the spin compensation cloud. We chose the impurity defined by the couplings $U' = 2$, $t' = 0.5$. In this case, since J_{eff} is large (as long as the relation $J_{eff} = 4t'^2/U'$ is applicable to these parameters), we expect a relatively small length ξ of the spin compensation cloud. In addition, the expression for the Kondo temperature for non-interacting leads ($U = 0$), $T_K = t'\sqrt{U'/(2t)}\exp\left(-\pi t U'/(8t'^2)\right)$, although not much precise for these impurity parameters, gives $T_K \approx 0.02$ which is reasonably accessible by SSE simulations. In Fig. 9(a) the spin compensation cloud $S(r)$ is shown at several temperatures for the case of non-interacting leads, $U = 0$. The temperature is in units of t, $k_B = 1$. It is remarkable the convergence of finite temperature results obtained with SSE to the zero temperature ones obtained with DMRG. Notice that both techniques are in principle exact but SSE results correspond to PBC systems while DMRG ones to OBC chains.

The length ξ is shown in Fig. 9(b). Errors were computed from the deviation of results obtained in four independent runs. For $T > T^*$, $T^* \approx 0.375$, ξ is equal to half the chain length, implying that the spin compensation cloud exceeds the limits of the chain. For $T < T^*$, ξ starts to be smaller than half the chain length indicating that now the cloud is fitting in the chain. That is to say, for $T < T^*$ the system manages to compensate the spin of the impurity but this is not possible for $T > T^*$. If the Kondo temperature is thought as the crossover temperature around which the impurity spin becomes compensated then T^* would be a measure of the Kondo temperature in finite systems, that is, $T^* = T^*(L)$. As mentioned in Section II, there is a certain degree of arbitrariness in the estimation of ξ because of the cutoff x but what is relevant is to determine how T^* behaves when a parameter of the system is varied. For the case of $U = 1$, T^* reduces its value to ≈ 0.25. This seems a trend as the correlations on the leads are increased but results for larger values of U have larger error bars and so they are not precise enough to confirm this trend.

V. CONCLUSIONS

In summary, we have studied the single-impurity Anderson-Hubbard model on finite chains with numerical techniques. In the first place, we analyzed how the reduction of the electron density from half-filling to quarter-filling affects the Kondo resonance for non-interacting leads. Physical quantities defining the magnetic character of the impurity show in general a weak behavior with the electron density except when the impurity is, at half-filling, close to a mixed valence regime. In this case there is a steep lost of magnetic character by reducing the density. This behavior is reflected also in the impurity LDOS and in the conductance in linear response. Next, we turn to the main topic of this work which is the study of the effects of a Hubbard interaction on the leads at quarter-filling. A very clear and interesting result is that U drives the impurity into a more defined Kondo regime (Fig. 5) although accompanied in most cases by a reduction of the spectral weight of the impurity LDOS. This reduction is however not general since for an impurity close to the mixed valence regime we observed a nonmonotonic behavior. As we mentioned in the Introduction, there is a number of strongly correlated materials which can be or have already been implemented[7] in nanoscopic devices and where some of the present results for the impurity LDOS could be contrasted. The conductance, computed for a small finite bias applied to the leads, follows the behavior of the impurity LDOS. For the impurities in a well-defined Kondo regime, the conduc-

tance is suppressed by U in finite chains, in agreement with what is expected for an impurity in a Luttinger liquid. Again, for the impurity close to a mixed valence regime, G increases for small U but eventually starts to decrease for large values of U. This nonmonotonic behavior indicates a complex interplay between the interactions on the impurity and the ones on the leads (in addition, of course, to the impurity-leads interactions).

Finally, we exploit one of the important advantages of the real space methods we used, that is, the possibility of getting a measure of the spin screening or compensation of the impurity. The "spin compensation cloud" gives an insight on the internal working of the Kondo effect and it does not depend just on properties at the impurity site but also on U on the leads. As shown in Fig. 6, finite-size effects are more important for small values if U. The proposed determination of the Kondo temperature in finite systems through the spin compensation cloud, has to be thoroughly explored as a function of density and coupling parameters. We emphasize that this numerical estimation of T^* is completely general in the sense that it is not limited to 1D Anderson-Hubbard model but could be used for any Hamiltonian for the leads, for example the Kondo lattice model, and also not limited to 1D leads, although beyond 1D the "minus sign problem" makes difficult the application of QMC methods. Moreover, we believe that the dependence of T^* with the finite size of the system could be experimentally measured and compared with theoretical results.

Acknowledgments

This work was supported in part by grant PICT 03-12409 (ANPCYT).

[1] D. Goldhaber-Gordon, H. Shtrikman, D. Mahalu, D. Abusch-Magder, U. Meirav, M. A. Kastner, Nature **391**, 156 (1998); S. M. Cronenwett, T. H. Oosterkamp, and L. P. Kouwenhoven, Science **281**, 540 (1998); W. G. van der Wiel, S. De Franceschi, T. Fujisawa, J. M. Elzerman, S. Tarucha, and L. P. Kouwenhoven, Science **289**, 2105 (2000).

[2] A. J. Hewson, *The Kondo problem to heavy fermions*, (Cambridge University Press, Cambridge, UK, 1993).

[3] S. A. Wolf, D. D. Awschalom, R. A. Buhrman, J. M. Daughton, S. von Molnár, M. L. Roukes, A. Y. Chtchelkanova, and D. M. Treger, Science **294**, 1488 (2001). S. Maekawa and T. Shinjo, *Spin Dependent Transport in Magnetic Nanostructures*. (Taylor & Francis, London, 2002).

[4] A. N. Pasupathy, R. C. Bialczak, J. Martinek, J. E. Grose, L. A. K. Donev, P. L. McEuen, and D. C. Ralph, Science **306**, 86 (2004); J. Nygaard, *et al*, cond-mat/0410467.

[5] P. Levy, A. G. Leyva, H. E. Troiani, and R. D. Sánchez, Appl. Phys. Lett. **83**, 5247 (2003).

[6] L. Krusin-Elbaum, D. M. Newns, H. Zeng, V. Derycke, J. Z. Sun, and R. Sandstrom, Nature **431**, 672 (2004).

[7] M. J. Biercuk, S. Garaj, N. Mason, J. M. Chow, C. M. Marcus, Nano Letters **5**, 1267 (2005).

[8] J. Nygaard, D. H. Cobden, and P. E. Lindelof, Nature **408**, 342 (2000).

[9] S. J. Tans, A. R. M. Verschueren, C. Dekker, Nature **393**, 49 (1998); K. Tsukagoshi, B. W. Alphenaar, H. Ago, Nature **401**, 572 (1999).

[10] M. Bockrath, D. H. Cobden, J. Lu, A. G. Rinzler, R. E. Smalley, L. Balents, and P. L. McEuen, Nature, **397**, 598 (1999).

[11] D. H. Lee and J. Toner, Phys. Rev. Lett. **69**, 3378 (1992); A. Furusaki and N. Nagaosa, Phys. Rev. Lett. **72**, 892 (1994).

[12] C. L. Kane and M. P. A. Fisher, Phys. Rev. B **46**, 7268 (1992).

[13] P. Simon and I. Affleck, Phys. Rev. B **68**, 115304 (2003).

[14] S. Andergassen, T. Enss, and V. Meden, Phys. Rev. B **73**, 153308 (2006).

[15] P. Schlottmann and A. A. Zviagin, Phys. Rev. B **67**, 115113 (2003).

[16] T. Hotta, M. Moraghebi, A. Feiguin, A. Moreo, S. Yunoki, and E. Dagotto, Phys. Rev. Lett. **90**, 247203 (2003).

[17] L. Balents and M. P. A. Fisher, Phys. Rev. B **55**, R11973 (1997).

[18] S. Costamagna and J. A. Riera, in preparation.

[19] D. J. Derro, E. W. Hudson, K. M. Lang, S. H. Pan, J. C. Davis, J. T. Markert, and A. L. de Lozanne, Phys. Rev. Lett. **88**, 097002 (2002).

[20] S. R. White, Phys. Rev. Lett. **69**, 2863 (1992); Phys. Rev. B **48**, 10345 (1993); U. Schollwöck, Rev. Mod. Phys. 77, 259 (2005).

[21] C. J. Gazza, M. E. Torio, and J. A. Riera, Phys. Rev. B **73**, 193108 (2006).

[22] J. E. Gubernatis, J. E. Hirsch, and D. J. Scalapino, Phys. Rev. B **35**, 8478 (1987).

[23] K. Hallberg and R. Egger, Phys. Rev. B **55**, 8646 (1996).

[24] A. W. Sandvik, Phys. Rev. B **59**, R14157 (1999).

[25] *Density-Matrix Renormalization*, edited by I. Peschel, X. Wang, M. Kaulke, and K. Hallberg (Springer, Berlin, 1999).

[26] K. A. Hallberg, Phys. Rev. B **52**, 9827 (1995); E. Jeckelmann, Phys. Rev. B **66**, 045114 (2002).

[27] A. E. Feiguin and S. R. White, Phys. Rev. B **72**, 020404(R) (2005).

[28] U. Schollwöck, J. Phys. Soc. Jpn. 74 (Suppl.), 246 (2005), and references therein.

[29] P. Schmitteckert, Phys. Rev. B **70**, 121302(R) (2004); D. Bohr, P. Schmitteckert, and P. Wölfle, Europhys. Lett., **73**, 246 (2006).

[30] K. A. Al-Hassanieh, A. E. Feiguin, J. A. Riera, C. A. Büsser, and E. Dagotto, Phys. Rev. B **73**, 195304 (2006).

[31] N. S. Wingreen, A. P. Jauho, and Y. Meir, Phys. Rev. B **48**, 8487 (1993).

[32] M. A. Cazalilla and J. B. Marston, Phys. Rev. Lett. **88**, 256403 (2002).

[33] S. R. White, I. Affleck, and D. J. Scalapino, Phys. Rev. B **65**, 165122 (2002); M. Mori, T. Tohyama, S. Maekawa, and J. A. Riera, Phys. Rev. B **69**, 014513 (2004).

[34] D. C. Langreth, Phys. Rev. **150**, 516 (1966).
[35] Y. Meir and N. S. Wingreen, Phys. Rev. Lett. **68**, 2512 (1992).
[36] H. J. Schulz, Phys. Rev. Lett. **64**, 2831 (1990).